

Complete spectra of the Dirac operator and their relation to confinement

Falk Bruckmann^a, Christof Gattringer^b and Christian Hagen^a

^a Institut für Physik, Universität Regensburg
93040 Regensburg, Germany

^b Institut für Physik, Universität Graz
8010 Graz, Austria

Abstract

We compute complete spectra of the staggered lattice Dirac operator for quenched SU(3) gauge configurations below and above the critical temperature. The confined and the deconfined phase are characterized by a different response of the Dirac eigenvalues to a change of the fermionic boundary conditions. We analyze the role of the eigenvalues in recently developed spectral sums representing the Polyakov loop. We show that the Polyakov loop gets its main contributions from the UV end of the spectrum.

To appear in Physics Letters B.

Introduction

In recent years many numerical studies of low lying eigenvalues and eigenvectors of lattice Dirac operators were published. The reason for analyzing low lying eigenvalues is twofold: Firstly, based on the Banks-Casher formula [1], a close connection of topological objects to the chiral condensate has been proposed [2]. Secondly, for low lying eigenvalues many results from random matrix theory are available and were tested numerically in detail.

While the low lying eigenvalues and their relation to chiral symmetry breaking are well analyzed, very little is known about the UV part of the spectrum and its possible connection to confinement. Partly this situation is due the fact that an evaluation of complete spectra of a lattice Dirac operator is a considerable numerical challenge.

A new way to analyze a possible relation between Dirac eigenvalues and confinement was proposed in [3]. It was shown that the Polyakov loop can be written as a linear combination of spectral sums over moments of Dirac eigenvalues computed with different (fermionic) boundary conditions. For the quenched case the Polyakov loop P is an order parameter for confinement, with $\langle P \rangle = 0$ in the confined phase, while in the deconfined phase (above T_c) the Polyakov loop develops a non-vanishing expectation value¹. In [3] it was speculated, that the difference between confined and deconfined phase can be characterized by a different response of the Dirac eigenvalues to changing boundary conditions. This difference leads to a non-vanishing $\langle P \rangle$ only in the deconfined phase.

In this letter we analyze whether this scenario can be established in a numerical study of complete spectra of the staggered lattice Dirac operator. Furthermore we address the question which part of the spectrum, IR or UV, contributes most to the Polyakov loop.

Spectral sums for the Polyakov loop

The spectral sums for the Polyakov loop, first presented in [3], were derived for the Wilson Dirac operator. Here we use the staggered Dirac operator at vanishing quark mass,

$$D(n, m) = \frac{1}{2} \sum_{\mu=1}^4 \eta_{\mu}(n) \left[U_{\mu}(n) \delta_{n+\hat{\mu}, m} - U_{\mu}(n - \hat{\mu})^{\dagger} \delta_{n-\hat{\mu}, m} \right], \quad (1)$$

where n and m are integer valued 4-vectors labeling the lattice sites and $\eta_{\mu}(n) =$

¹In the theory with dynamical fermions one could study correlators of Polyakov loops to analyze the static potential.

$(-1)^{n_1+\dots+n_{\mu-1}}$ is the staggered sign function. The $U_\mu(n)$ denote the SU(3)-valued gauge links and we have set the lattice spacing to $a = 1$.

We use an $L^3 \times N$ lattice and require that the number N of lattice points in time direction (the 4-direction) is even. As it stands, the Dirac operator has periodic boundary conditions in all directions. Below we will also need temporal boundary conditions with a phase z or its complex conjugate phase z^* . These are implemented by multiplying the last temporal links with z and z^* , i.e., $U_4(\vec{n}, n_4 = N) \rightarrow z U_4(\vec{n}, n_4 = N)$ or $U_4(\vec{n}, n_4 = N) \rightarrow z^* U_4(\vec{n}, n_4 = N)$. Here we make the particular choice of Z_3 -valued boundary conditions and set $z = e^{i2\pi/3}$. We consider the Polyakov loop averaged over all of space,

$$P = \frac{1}{L^3} \sum_{\vec{n}} \text{Tr}_c \left[\prod_{n_4=1}^N U_4(\vec{n}, n_4) \right], \quad (2)$$

where Tr_c denotes the trace over the color indices.

Following the arguments in [3], one finds that the Polyakov loop is given by a linear combination of spectral sums,

$$P = \frac{2^N}{3NL^3} \left[\sum_i (\lambda^{(i)})^N + z^* \sum_i (\lambda_z^{(i)})^N + z \sum_i (\lambda_{z^*}^{(i)})^N \right]. \quad (3)$$

Each sum runs over all $3L^3N$ eigenvalues and $\lambda^{(i)}$, $\lambda_z^{(i)}$, and $\lambda_{z^*}^{(i)}$ denote the eigenvalues computed with periodic, z -valued, and z^* -valued boundary conditions respectively. The Polyakov loop P thus is represented as a linear combination of spectral sums for the N -th power of the eigenvalues computed with three different fermionic boundary conditions in time direction. The boundary conditions for the gauge fields are always kept periodic.

It is interesting to note, that exact zero modes do not contribute to the spectral sum for the Polyakov loop. Thus, isolated topological objects which give rise to a zero mode, do not play a role for building up the expectation value of the Polyakov loop².

We stress that the result (3) is an exact formula for the Polyakov loop of an arbitrary gauge configuration. Below we will study numerically the expectation value $\langle P \rangle$ of the Polyakov loop in a quenched ensemble. The r.h.s. of (3) then is rewritten in terms of expectation values of the N -th moments of Dirac eigenvalues computed with the three different boundary conditions,

$$\langle P \rangle = \frac{2^N}{3NL^3} \sum_i \left[\langle (\lambda^{(i)})^N \rangle + z^* \langle (\lambda_z^{(i)})^N \rangle + z \langle (\lambda_{z^*}^{(i)})^N \rangle \right]. \quad (4)$$

²We remark that the staggered Dirac operator does not have exact zero modes, but for sufficiently smooth configurations the would-be zero modes can be identified relatively clearly and are very close to the origin [4].

This formula relates the vacuum expectation value of the Polyakov loop, which originally is a purely gluonic quantity, to spectral sums of the Dirac eigenvalues. Since the Polyakov loop is an order parameter for confinement (in the quenched case), with $\langle P \rangle = 0$ in the confined phase ($T < T_c$) and $\langle P \rangle \neq 0$ in the deconfined phase ($T > T_c$), the formula (4) allows to study the relation of confinement and the spectrum of the Dirac operator.

As one crosses the critical temperature into the deconfined phase, $\langle P \rangle$ acquires a non-vanishing expectation value. Equation (4) implies that the response of the eigenvalues to the boundary conditions has to change at T_c , such that the spectral sums on the right-hand side do no longer cancel and $\langle P \rangle \neq 0$. In the subsequent sections we study the response of the eigenvalues to changing boundary conditions and explore which parts of the Dirac spectrum give the main contributions to the spectral sums.

Distribution of the Dirac eigenvalues and their response to changing boundary conditions

For a numerical study of the formula (4) we need to compute complete spectra of the Dirac operator using three different boundary conditions. Since a numerical evaluation of all eigenvalues is a demanding task we are restricted to relatively small lattices. Here we use quenched gauge field configurations generated with the Lüscher-Weisz action [5] on lattices of size $6^3 \times 4$.

We work with two different values of the inverse coupling, $\beta = 7.6$ and $\beta = 8.0$. Setting the scale with the Sommer parameter one finds lattice spacings of $a = 0.194(4)$ fm and $a = 0.135(1)$ fm for the two couplings [6]. With a temporal extension of $N = 4$ this corresponds to temperatures of $T = 254$ MeV for $\beta = 7.6$, and $T = 364$ MeV for $\beta = 8.0$. Thus, we have two ensembles with temperatures below and above the QCD phase transition which for the quenched case is at $T_c \sim 300$ MeV. Using LAPACK routines we compute complete spectra of the staggered Dirac operator with the three boundary conditions for 2000 configurations from each of the two ensembles. The statistical errors we quote for the averaged observables are evaluated with single elimination Jackknife.

We begin the presentation of our numerical results with a discussion of the eigenvalue distribution. Since the massless staggered Dirac operator is an anti-hermitian matrix, it has eigenvalues on the imaginary axis. We order these with respect to their absolute value and the sign of the imaginary part (the eigenvalues come in complex conjugate pairs). For analyzing the distribution of the eigenvalues we divide $|\lambda|$ into small bins of size $\Delta|\lambda|$ and count the number of eigenvalues, Δn , in each of the bins. In Fig. 1 we plot $\Delta n / \Delta|\lambda|$ as a function of $|\lambda|$ for both ensembles below and above T_c (see [7] for a similar analysis in

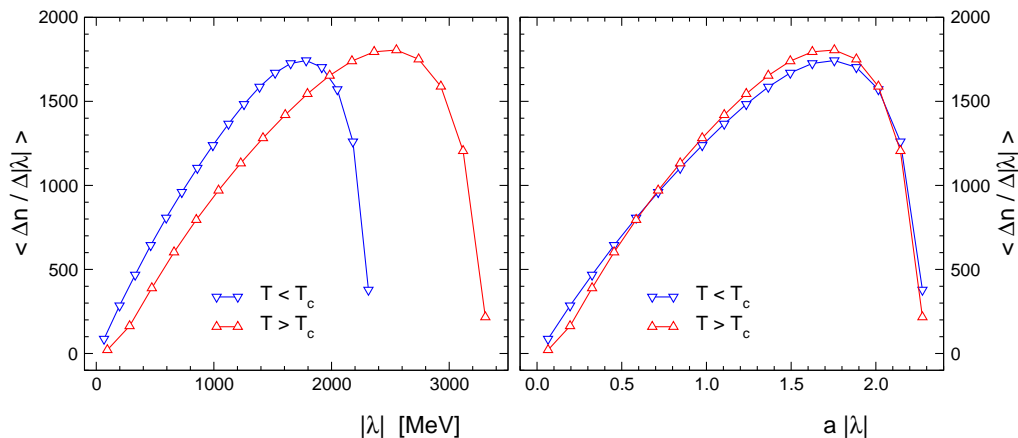


Figure 1: Distribution of the eigenvalues λ as a function of $|\lambda|$ (for periodic b.c.). In the l.h.s. plot we use MeV as unit for the eigenvalues, while on the r.h.s. the dimensionless quantity $a|\lambda|$ (lattice units) is plotted on the horizontal axis.

the case of SU(2)). On the horizontal axis we use either physical units (l.h.s. plot), or the dimensionless combination $a|\lambda|$ (r.h.s.).

As can be seen from the r.h.s. plot, the curves for the distribution of the eigenvalues are very similar for the two ensembles when plotted in lattice units. At small $|\lambda|$ the density of eigenvalues is a little bit depleted for the ensemble with $T > T_c$. This can be understood qualitatively from the Banks-Casher formula [1], which predicts a vanishing spectral density at the origin for the chirally symmetric phase (above T_c). The corresponding opening of a spectral gap is well documented in numerical studies [8] and this phenomenon is reflected in the lower density at small $|\lambda|$ seen in our data for $T > T_c$. The area under the two curves has to be equal (= the total number of eigenvalues) and we observe a light enhancement of the density for the $T > T_c$ spectra near the maximum. When we use physical units on the horizontal scale (l.h.s. plot), the two densities are stretched with different factors due to the different lattice spacing for the two values of the coupling we use.

It is obvious that the distribution of the eigenvalues plays an important role for the spectral representation (4). Energy ranges where the density of eigenvalues is large will in general be more important than those parts of the spectrum with a low density. In order to disentangle the role of the density from other aspects, such as the response to changing boundary conditions, we now study two observables for individual eigenvalues.

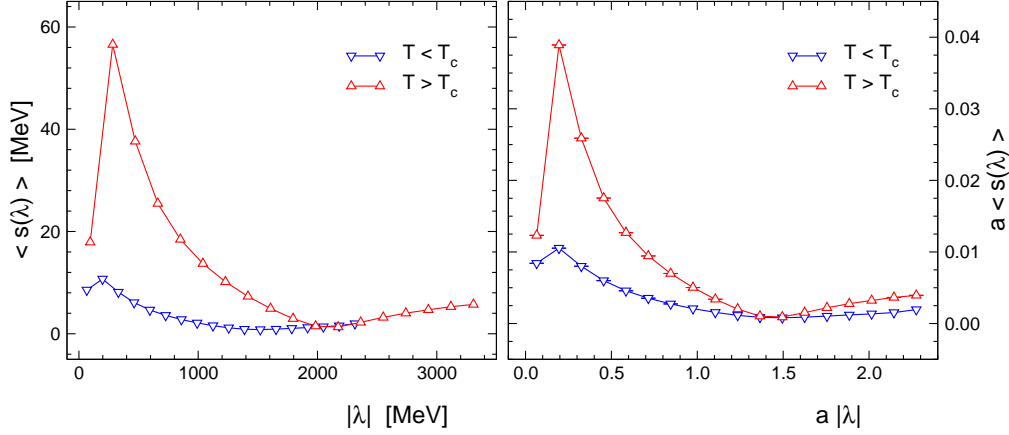


Figure 2: Average shift of the eigenvalues when changing the boundary condition of the Dirac operator, plotted as a function of $|\lambda|$. In the l.h.s. plot physical units are used and lattice units on the r.h.s.

The first property of the eigenvalues we consider is their average shift when the boundary conditions are changed. To quantify this effect we define the average shift $s(\lambda^{(i)})$, by comparing an eigenvalue $\lambda^{(i)}$ for periodic boundary conditions to its partners $\lambda_z^{(i)}$ and $\lambda_{z^*}^{(i)}$, computed with z - and z^* -boundary conditions,

$$s(\lambda^{(i)}) = \left(|\lambda^{(i)} - \lambda_z^{(i)}| + |\lambda^{(i)} - \lambda_{z^*}^{(i)}| + |\lambda_z^{(i)} - \lambda_{z^*}^{(i)}| \right) / 3. \quad (5)$$

In Fig. 2 we show the average shift $s(\lambda)$ as a function of $|\lambda|$, again using physical units on the l.h.s. plot and lattice units on the r.h.s. The most obvious feature of the plots is the fact that the shift of the eigenvalues is considerably stronger for the $T > T_c$ ensemble, in particular towards the IR end of the spectrum. This confirms an observation made in [9], where it was shown, that for $T > T_c$ the size of the spectral gap strongly depends on the fermionic boundary condition. The plots furthermore show, that for $T > T_c$ the shift is stronger than for the data at $T < T_c$, not only in the deep IR, but for all of the eigenvalues.

Apart from the different total shift, the two ensembles display also common features: A clear maximum close to the IR end, a minimum for midrange values and another increase at the UV end. The plots demonstrate that the IR modes are shifted most, combined with a less pronounced shift of the largest eigenvalues. It is interesting to note that the parts of the spectrum with large shifts coincide with low densities (compare Fig. 1).

Finally, we remark that both curves show a drop for the first bin in the IR.

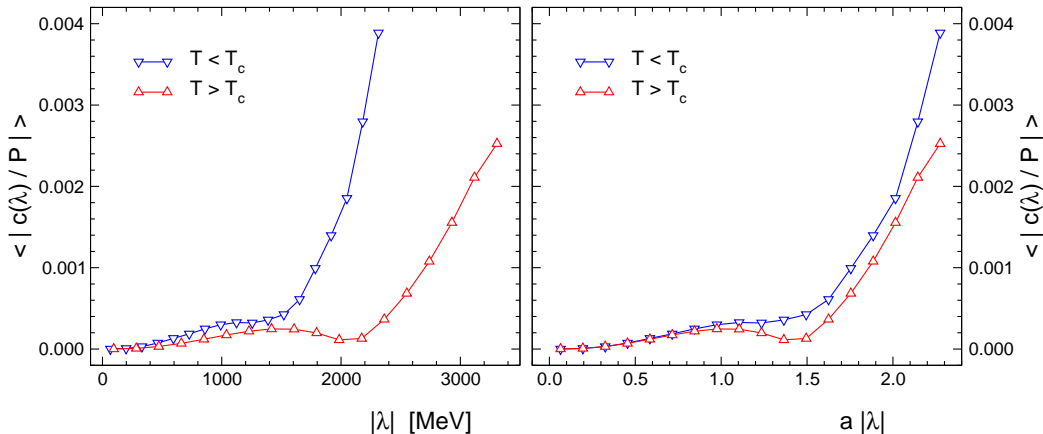


Figure 3: Contribution of an eigenvalue to the spectral sum for the Polyakov loop, as a function of $|\lambda|$ (l.h.s. plot: physical units, r.h.s. plot: lattice units).

We attribute this to the would-be zero modes which are stabilized by topology and thus should not move at all. However, since the staggered Dirac operator has only approximate zero modes, these eigenvalues move a little bit, but considerably less than the bulk modes, thus creating the drop in the lowest bin.

Contributions to the Polyakov loop

We have demonstrated that when changing the boundary conditions, different parts of the spectrum are shifted by different amounts. However, in the formula (4) for the Polyakov loop the N -th powers of the eigenvalues enter and the shifted spectra are weighted with the phases z and z^* . Thus, we now consider the contribution $c(\lambda^{(i)})$ of an individual eigenvalue to the spectral sum,

$$c(\lambda^{(i)}) = \frac{2^N}{3NL^3} \left[(\lambda^{(i)})^N + z^* (\lambda_z^{(i)})^N + z (\lambda_{z^*}^{(i)})^N \right]. \quad (6)$$

In Fig. 3 we show the absolute value of the contribution $c(\lambda)$ normalized by the total Polyakov loop³ as a function of $|\lambda|$. For both ensembles the size of the contribution increases strongly towards the UV end of the spectrum. Furthermore, when plotted in lattice units (r.h.s. plot), the two curves show a similar behavior. They both start out with a modest slope which, after a small dip (or shoulder) near $a|\lambda| \sim 1.5$, turns into a steeper ascent. Fig. 3

³We remark, that on a finite lattice the Polyakov loop does not vanish exactly also below T_c . However, this “microscopic value” vanishes in the thermodynamic limit.

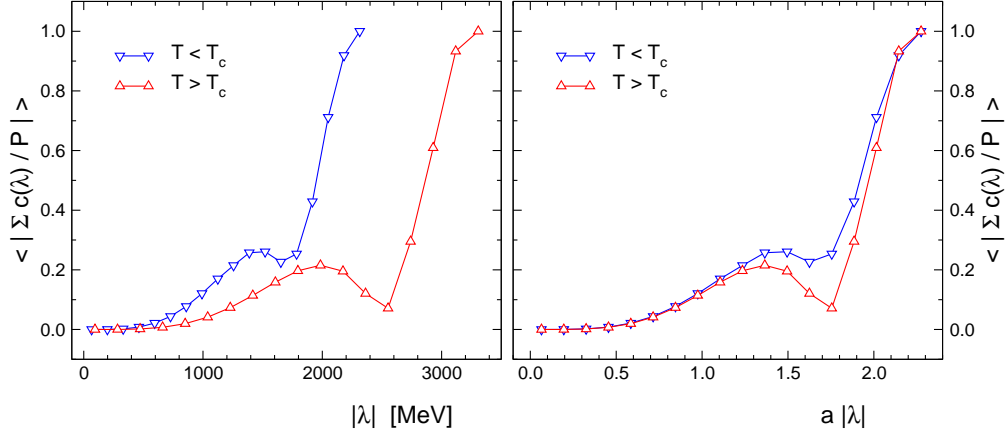


Figure 4: Accumulated contribution to the spectral sum for the Polyakov loop, as a function of $|\lambda|$ (l.h.s. plot: physical units, r.h.s. plot: lattice units).

demonstrates, that although according to the last plot the IR modes are shifted more, the UV modes have a larger contribution to the Polyakov loop.

Having studied the contribution of the individual modes, we finally have to fold in also the distribution of the eigenvalues analyzed in Fig. 1. To take the spectral density into account we compute the accumulation of the contributions $c(\lambda)$, by summing all contributions up to a given value of $|\lambda|$, i.e., we analyze the cumulated quantity $\sum_{|\lambda'| \leq |\lambda|} c(\lambda')$. In Fig. 4 we plot the absolute value of this quantity, normalized with the total Polyakov loop, as a function of $|\lambda|$. As was to be expected, the IR modes do not contribute a lot and most of the Polyakov loop is carried by the UV modes. What is somewhat surprising, is the fact that the cumulation is not a monotonically increasing function, but has a dip which is particularly pronounced for $T > T_c$. This shows that the buildup of the Polyakov loop from the spectral sums is not a simple linear process. The r.h.s. plot demonstrates that, when plotted in lattice units, the curves for the two ensembles are rather similar, as could already be concluded from the similarity of the behavior of the corresponding curves in Figs. 1 and 3. We remark that at the UV end both curves reach 1.0 to machine precision, which is a good check that the exact formulas (3), (4) were implemented correctly.

Phase of the Polyakov loop above T_c

Above T_c the phase of the Polyakov loop has values close to the angles of the group center, i.e., close to 0 , $2\pi/3$ and $4\pi/3$. This can be seen in the plot on the very right in Fig. 5 where we show the complete spectral sum for the

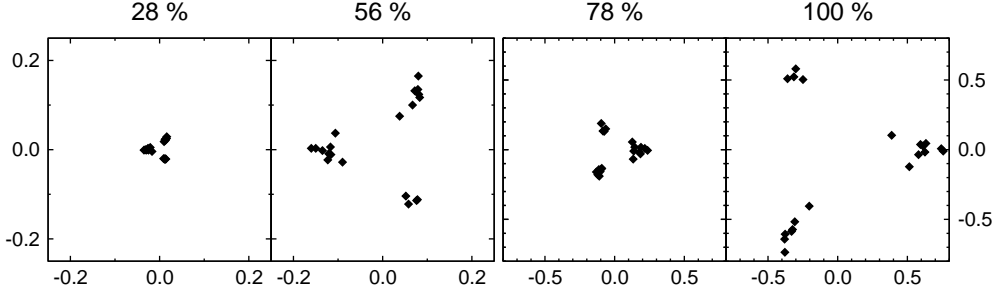


Figure 5: The Polyakov loop in the complex plane for 20 configurations above T_c as reconstructed from the spectral sums with 28%, 56%, 78% and 100% of the eigenvalues (left to right). Note that the two plots on the l.h.s. have a different scale.

Polyakov loop for 20 gauge configurations. For the truncated sum, we observe a surprising phenomenon: When including less than roughly two thirds of the eigenvalues, one finds that the results for the Polyakov loop show a phase shift of 180 degrees (see the two plots on the l.h.s. of Fig. 5). Only the largest third of the eigenvalues has the correct phase and, since the UV contributions dominate, determine the final phase (the two plots on the r.h.s. of Fig. 5).

In Fig. 6 we show the phase shift $\Delta\phi$ of the truncated spectral sum relative to the phase of the full sum. It is obvious, that when truncating the sum at less than two thirds of the eigenvalues, the phase is shifted by a value of 180 degrees (i.e., a shift of π), and only the UV eigenvalues drive the relative shift to zero.

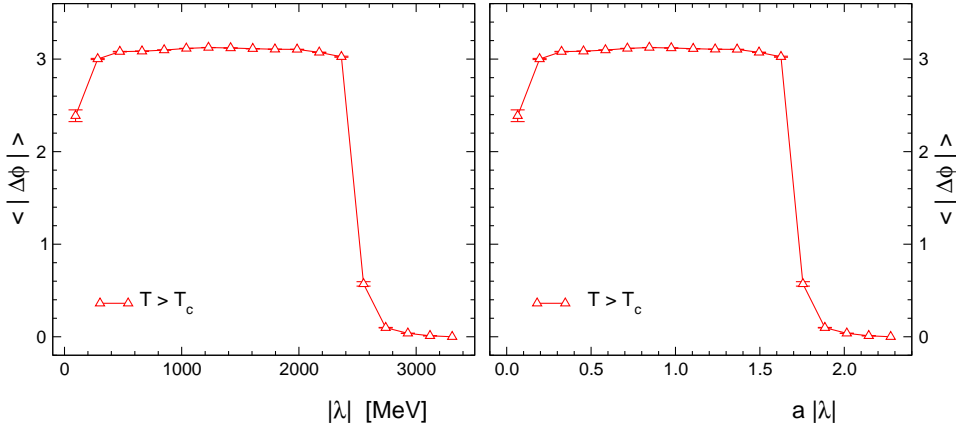


Figure 6: Phase shift of the truncated spectral sums for the Polyakov loop.

It is interesting to note, that the position where the phase starts to come out right coincides with the position of the dip observed in Fig. 4. To summarize, the truncated sum for every configuration first evolves in the opposite direction in the complex plane and after two thirds turns back to approach the correct full Polyakov loop.

Summary and interpretation

We have generalized the discussion of spectral sums of Dirac eigenvalues representing the Polyakov loop [3] to the case of the staggered Dirac operator. In order to study these spectral sums numerically we computed complete Dirac spectra with three different fermionic boundary conditions, using quenched ensembles below and above the QCD phase transition.

Different aspects of these spectra were studied, in particular the distribution of the eigenvalues and their shift under a change of boundary conditions were analyzed. Concerning this shift we established that the IR modes are shifted most and also towards the UV end found a small increase. A comparison with the results from the distribution analysis showed that the eigenvalues with largest shift coincide with the regions of lowest eigenvalue density. Qualitatively this pattern holds for both ensembles, but for $T > T_c$ the shift of the eigenvalues is considerably larger than for $T < T_c$. This enhanced response to changing boundary conditions leads to a non-vanishing $\langle P \rangle$ for $T < T_c$, while in the confined phase only a microscopic value of $\langle P \rangle$ emerges which vanishes in the thermodynamic limit.

Concerning the buildup of the Polyakov loop, we considered the contribution of an individual eigenvalue as well as the accumulated contribution. The contribution of individual eigenvalues does not take into account that the density of the eigenvalues is a function of their size and thus disentangles the two effects of a varying density and the different contribution of individual eigenvalues. Both the individual as well as the accumulated contributions show that mainly the eigenvalues in the UV build up the Polyakov loop. For the phase of the accumulated contribution we have shown that in the IR a phase shift of 180 degrees is observed which vanishes at the UV end.

We have established the following qualitative scenario for the relation between Dirac eigenvalues and the Polyakov loop below and above T_c : In both phases the eigenvalues respond to changing the boundary conditions, but the response is considerably larger in the deconfined phase. As a consequence, the linear combination of the spectral sums with different boundary conditions leads to $\langle P \rangle > 0$ in that case. Concerning the role of different eigenvalues, we find that the spectral sums for $\langle P \rangle$ are dominated by the UV end of the spectrum.

Acknowledgments: We thank Stefan Keppeler, Christian Lang, Andreas Schäfer, Erhard Seiler, Kim Splittorff, Jac Verbaarschot, Tilo Wettig and Andreas Wipf for interesting discussions. This work is supported by BMBF.

References

- [1] T. Banks and A. Casher, Nucl. Phys. B 169 (1980) 103.
- [2] D. Diakonov and V.Y. Petrov, Phys. Lett. B 147 (1984) 351; Nucl. Phys. B 272 (1986) 457; D. Diakonov, Talk given at International School of Physics, 'Enrico Fermi', Course 80: Selected Topics in Nonperturbative QCD, Varenna, Italy, 1995, hep-ph/9602375; T. Schäfer and E.V. Shuryak, Rev. Mod. Phys. 70 (1998) 323.
- [3] C. Gattringer, Phys. Rev. Lett. 97 (2006) 032003.
- [4] E. Follana, A. Hart and C. T. H. Davies [HPQCD Collaboration], Phys. Rev. Lett. 93 (2004) 241601; S. Dürr, C. Hoelbling and U. Wenger, Phys. Rev. D 70 (2004) 094502.
- [5] M. Lüscher and P. Weisz, Commun. Math. Phys. 97 (1985) 59, Err.: 98 (1985) 433; G. Curci, P. Menotti, and G. Paffuti, Phys. Lett. B 130 (1983) 205, Err.: B 135 (1984) 516.
- [6] C. Gattringer, R. Hoffmann and S. Schaefer, Phys. Rev. D 65 (2002) 094503.
- [7] M. E. Berbenni-Bitsch et al, Phys. Rev. Lett. 80 (1998) 1146.
- [8] C. Gattringer *et al.*, Nucl. Phys. B 617 (2001) 101, Nucl. Phys. B 618 (2001) 205.
- [9] C. Gattringer and S. Schaefer, Nucl. Phys. B 654 (2003) 30; C. Gattringer, P. E. L. Rakow, A. Schäfer and W. Söldner, Phys. Rev. D 66 (2002) 054502.